

Cite this: *J. Mater. Chem. C*, 2018,
6, 3613

Effects of *meso*-M(PPh₃)₂Cl (M = Pd, Ni) substituents on the linear and third-order nonlinear optical properties of chalcogenopyrylium-terminated heptamethines in solution and solid states†‡

Iryna Davydenko,^{id}^a Sepehr Benis,^{id}^b Stephen B. Shiring,^{id}^a Janos Simon,^a
Rajesh Sharma,^{id}^{bc} Taylor G. Allen,^{id}^a San-Hui Chi,^{id}^a Qing Zhang,^a
Yulia A. Getmanenko,^{id}^a Timothy C. Parker,^{id}^a Joseph W. Perry,^{id}^a
Jean-Luc Brédas,^{id}^a David J. Hagan,^{id}^b Eric W. Van Stryland,^{id}^b
Stephen Barlow^{id}^a and Seth R. Marder^{id}^{*a}

Aggregation of cyanine-like dyes can significantly affect their optical properties. Here we report the effects of bulky *meso*-M(PPh₃)₂Cl (M = Pd, Ni) substitution on the molecular and solid-state optical characteristics of chalcogenopyrylium-terminated heptamethines. Metallated dyes were synthesised by reaction of the *meso*-chloro dyes with Pd(PPh₃)₄ or Ni(PPh₃)₄ at room temperature. The two PPh₃ ligands are *trans* and the plane formed by the metal atom and its ligands is approximately orthogonal to that of the polymethine π -system. Replacement of Cl by M(PPh₃)₂Cl leads to a large blue shift of the solution absorption maximum and a decrease in the associated transition dipole moment, these effects being slightly more pronounced for Ni than for Pd. DFT calculations and electrochemical data suggest the blue shifts can largely be attributed to destabilisation of the LUMO by the more strongly π -donating M(PPh₃)₂Cl groups. The magnitude of the real part of the molecular third-order polarisability, $\text{Re}(\gamma)$, decreases in the order Cl > Pd(PPh₃)₂Cl >> Ni(PPh₃)₂Cl. Within the framework of the sum-over-states expression for $\text{Re}(\gamma)$, the difference between Cl and Pd(PPh₃)₂Cl examples can be rationalised considering the effects of the $S_0 \rightarrow S_1$ transition energy and transition dipole moment on the two-state term associated with $S_0 \rightarrow S_1$. On the other hand, the magnitude of $\text{Re}(\gamma)$ for a Ni(PPh₃)₂Cl dye is anomalously low; SAC-Cl/HF/cc-pVDZ excited-state calculations reveal this is due to a two-photon-allowed S_2 state at unusually low energy for a cyanine-like dye, leading to a large positive three-state contribution to γ opposing the negative two-state S_1 term. Thus, despite a cyanine-like molecular structure and linear absorption spectrum, this compound does not exhibit cyanine-like nonlinear optical behavior. Turning to the effects on aggregation, molecular dynamics simulations suggest that Pd(PPh₃)₂Cl substitution largely suppresses H- and J-aggregate formation; indeed experimental absorption spectra for neat films of Pd(PPh₃)₂Cl-substituted dyes are fairly similar to corresponding solution spectra. A 50 wt% blend of a Pd(PPh₃)₂Cl-substituted telluropyrylium-terminated dye with amorphous polycarbonate exhibits a third-order susceptibility of -3×10^{-11} esu, a two-photon figure-of-merit in excess of 10, and linear loss of 6.3 dB cm^{-1} , which are close to the requirements for all-optical switching applications.

Received 6th November 2017,
Accepted 5th December 2017

DOI: 10.1039/c7tc05050j

rsc.li/materials-c

^a School of Chemistry and Biochemistry and Center for Organic Photonics and Electronics, Georgia Institute of Technology, Atlanta, Georgia 30332-0400, USA.
E-mail: seth.marder@chemistry.gatech.edu

^b CREOL, The College of Optics and Photonics, University of Central Florida, Orlando, Florida 32816, USA

^c Department of Physics, University Institute of Sciences, Chandigarh University, Mohali, Punjab 140413, India

† We dedicate this paper to the memory of the late Prof. Alexei I. Tolmachev who made many contributions to the chemistry of polymethine dyes including thiopyrylium-terminated examples, and to Prof. Fred Wudl in celebration of 50 years of his contributions to the materials chemistry of π -conjugated organics.

‡ Electronic supplementary information (ESI) available: Synthesis and characterisation; additional absorption spectra; TGA data; details of quantum-chemical calculations; and measurement details for NLO data and linear optical loss. See DOI: 10.1039/c7tc05050j

Introduction

Many cyanine-like polymethine dyes form aggregates in the solid state or in concentrated solid or liquid solutions;¹ their very large polarisabilities lead to strong van der Waals attractions that can outweigh electrostatic repulsions between like-charged dyes. J-aggregates have long played an important sensitising role in the silver halide photographic process,² while their strongly emissive properties have led to use in biological imaging³ and as probes of internanoparticle interactions.⁴ Broadening of absorption by the presence of

H-like aggregates may be beneficial in light-harvesting applications.⁵ However, in other applications, dye-dye interactions can be detrimental. In particular, although the molecular-level properties of cyanine-like dyes are attractive for third-order nonlinear optical (NLO) applications, especially all-optical switching (AOS) applications that rely on the nonlinear refractive index, these properties can be dramatically modified by aggregation.⁶

For AOS applications, (i) the real part of the third-order susceptibility, $\text{Re}(\chi^{(3)})$, at the wavelength of interest should be large in magnitude; (ii) nonlinear optical losses from two-photon absorption (2PA) should be small, *i.e.*, the imaginary part of third-order susceptibility, $\text{Im}(\chi^{(3)})$, should be minimised; and (iii) linear optical losses from one-photon absorption (1PA) and/or scattering should be low.⁷⁻⁹

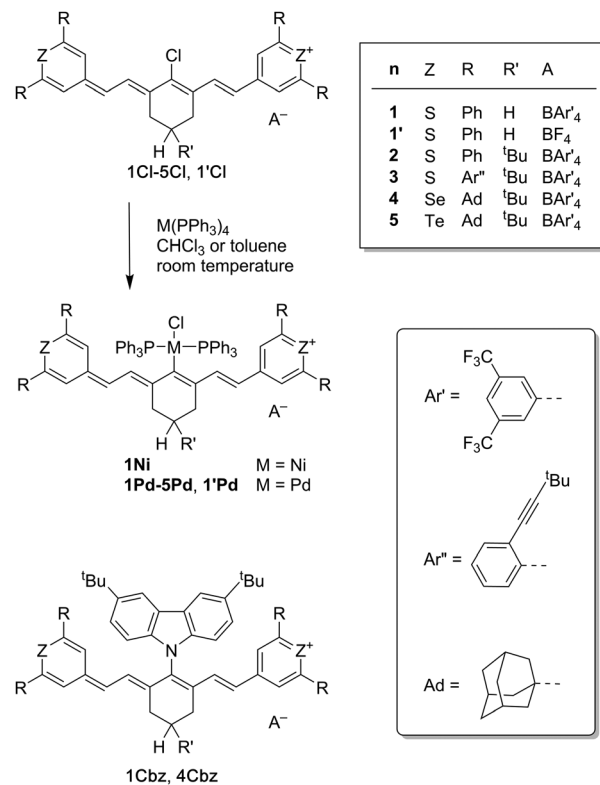
Perturbation theory allows the complex frequency-dependent susceptibility to be expressed using a “sum-over-states-expression”. The static (zero-frequency) real part of the third-order polarisability, $\text{Re}(\gamma_0)$ – the molecular quantity corresponding to $\text{Re}(\chi_0^{(3)})$ – is given by

$$\text{Re}(\gamma_0) \propto - \left(\frac{\mu_{\text{ge}}^4}{E_{\text{ge}}^3} \right)_{\text{“N”}} + \left(\frac{\mu_{\text{ge}}^2 \Delta\mu_{\text{ge}}^2}{E_{\text{ge}}^3} \right)_{\text{“D”}} + \sum_{e'} \left(\frac{\mu_{\text{ge}}^2 \mu_{\text{ee}'}^2}{E_{\text{ge}}^2 E_{\text{ee}'}} \right)_{\text{“T”}} \quad (1)$$

where μ , $\Delta\mu$, and E denote transition dipole moments, changes in state dipole moment, and transition energies, respectively, and subscripts g, e, and e' denote ground, first excited, and higher-lying excited states, respectively.^{10,11}

Typical cyanine-like polymethines generally exhibit large negative $\text{Re}(\gamma_0)$ due to a large negative “N” term, and relatively small positive “D” and “T” terms. The large “N”-term arises due to the strong (high- μ_{ge}) low-energy (small E_{ge}) 1PA-allowed S_0 - S_1 transition. Although such symmetrical cyanines have C_{2v} symmetry, they are quasi-linear and, thus, almost centrosymmetric; accordingly $\Delta\mu_{\text{ge}}$, and consequently the “D”-term contributions, are insignificant. Finally, the strongly 2PA-allowed (e') states of cyanine-like dyes are well separated in energy from S_1 ($E_{\text{ge}'} \gg E_{\text{ge}}$); resulting in “T”-terms that are small relative to the “N”-term.⁶

Moreover, besides large $|\text{Re}(\gamma_0)|$, cyanines exhibit several other optical properties potentially well suited to AOS. The well-spaced excited states and the narrow absorption bands mean that one can choose a dye for which E_{ge} is only a little higher than the photon energy of interest, $h\nu$. By carefully choosing the dye and photon-energy combination, one can potentially exploit near-resonance enhancement of $\text{Re}(\gamma_0)$ (which is maximised as $h\nu$ approaches E_{ge}) without incurring either linear loss through 1PA into S_1 ; 2PA into S_2 (*i.e.*, $2h\nu < E_{\text{ge}'}$), or vibronically assisted 2PA into S_1 ($2h\nu > E_{\text{ge}}$). For AOS at telecommunications wavelengths (1.3–1.55 μm), these criteria can be met by choosing dyes with $S_0 \rightarrow S_1$ absorptions at *ca.* 700–1200 nm. Chain length and/or the charge-stabilising terminal groups can be used to engineer absorptions into this range,¹² although very long-chain polymethines can exhibit “symmetry-breaking” phenomena, whereby they no longer exhibit cyanine-like spectra.¹³⁻¹⁷ Chalcogenopyrylium-terminated



Scheme 1 Synthesis of $\text{M}(\text{PPh}_3)_2\text{Cl}$ -functionalised chalcogenopyrylium-terminated heptamethines and related structures discussed in this work.

polymethines^{16,18-22} exhibit some of the lowest-energy absorptions for a given chain length, and heptamethines such as **1'Cl** (Scheme 1) have particularly promising solution linear and nonlinear optical properties for AOS.²³

However, high-chromophore density films are required for practical applications and the aggregation that occurs under such conditions can lead to broadening of the absorption bands and to the creation of new states,²⁴ both of which can impair the 1PA and 2PA transparency, as well as lead to light scattering. We have attempted to suppress aggregation effects in chalcogenopyrylium-terminated polymethines using Fréchet-type dendrons, but with only limited success.²⁵ More effective is the incorporation of moderately large but out-of-plane organic substituents in “end” (R in Scheme 1), “back” (R'), and “front”, *i.e.*, *meso*, substituents; some of these dyes, such as **4Cbz** (Scheme 1), exhibited an unprecedented combination of large $|\text{Re}(\chi^{(3)})|$, large $|\text{Re}(\chi^{(3)})/\text{Im}(\chi^{(3)})|$, and small linear optical loss at 1.55 μm .^{26,27} The substituents and counterion used also resulted in good solubility in low-polarity high-index solvents suitable for liquid-core optical fiber applications.²⁸

Recently we have found that $\text{Pd}(\text{PPh}_3)_2\text{Cl}$ groups can be rather easily introduced into the *meso*-positions of a variety of polymethine dyes by treatment of the corresponding Cl-substituted dyes with $\text{Pd}(\text{PPh}_3)_4$, and that these groups are very effective in disrupting intermolecular π -interactions, as demonstrated crystallographically, by absorption spectra of films, and for an anionic dye, by third-order NLO measurements.²⁹ Similar reactions may be used to introduce bulky palladium-based

substituents to perylene diimide^{29,30} or BODIPY³¹ cores, also leading to suppression of π -stacking in the solid state.

Here we apply the same metallation reaction to *meso*-chloro chalcogenopyrylium-terminated heptamethines (Scheme 1). We experimentally and theoretically compare the effects of Cl, Pd(PPh₃)₂Cl, and Ni(PPh₃)₂Cl substituents on molecular-level linear and nonlinear optical properties, and then examine the impact of these bulky *meso*-groups on intermolecular interactions. Finally we show that one example exhibits promising optical properties for AOS in a high-chromophore density film.

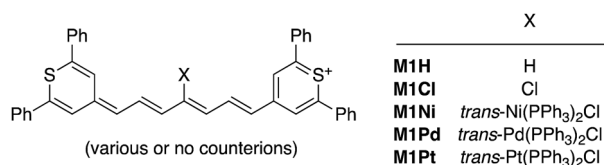
Results and discussion

Synthesis

As in our previous report on other classes of heptamethines,²⁹ Pd(PPh₃)₂Cl-substituted dyes could be obtained from the room-temperature reaction³² of the corresponding *meso*-chloro dyes with Pd(PPh₃)₄ (Scheme 1) under inert atmosphere, followed by column chromatography on silica gel. The Cl-precursor **1Cl** is commercially available (as IR1061); the other chloro dyes were obtained either by counterion metathesis (**1Cl**²³) or by condensation of the appropriate 4-methylchalcogenopyrylium salt (some of which are previously reported^{26,33,34} and others of which were newly synthesised) and the appropriate *meso*-chloro-substituted aniline-terminated pentamethine,²⁹ again followed by counterion metathesis (see ESI† for details).

One example of a Ni(PPh₃)₂Cl derivative, **1Ni**, was obtained in an analogous way using Ni(PPh₃)₄; although less thermally stable (see ESI†) than **1Pd**, this compound could still be obtained in good yield after purification by column chromatography. Extension of the reaction to Pt(PPh₃)₄ was more challenging: although an absorption attributable to a trace of the desired product was observed in the UV-vis-NIR spectrum of the crude material, the dye could not be isolated.

The ³¹P NMR spectra of **1Pd**, **1Pd** and **1Ni** exhibit a single resonance, whereas those of **2-4Pd** show a pair of doublets characterised by a coupling constant (J_{PP}) of ca. 300–400 Hz.³⁵ These observations suggest a *trans* arrangement of the phosphine ligands³⁶ and that the plane formed by the metal atom and its ligands is roughly orthogonal to that of the polymethine dye (the two phosphines being inequivalent in **2-4Pd** due to the presence of the ^tBu substituent); this is fully consistent with NMR and crystallographic data for other Pd(PPh₃)₂Cl-functionalised polymethines in our previous study,²⁹ and with DFT (ω B97X-D/cc-pVDZ) geometry optimisations for **M1Pd** and **M1Ni** (Scheme 2) in the present work.



Scheme 2 Structures examined computationally in this work.

Solution spectra

Absorption spectra for the metallated dyes and their chloro precursors were acquired in chloroform solution. All exhibit a strong and narrow cyanine-like feature, with a pronounced vibronic shoulder, in the near-IR, and only relatively weak absorption features in the visible. The variations in absorption maxima, λ_{\max} , for the **1-5Pd** series follow those in the corresponding **1-5Cl** species (see discussion below), but λ_{\max} for each of the Pd(PPh₃)₂Cl derivatives synthesised is hypsochromically shifted by ca. 600 cm⁻¹ relative to that of its Cl precursor (see Table S1, ESI†). The Ni(PPh₃)₂Cl derivative, **1Ni**, exhibits an even larger hypsochromic shift of ca. 750 cm⁻¹ relative to **1Cl**. These blue shifts (Fig. 1 and Table 1) are consistent with those seen in our previous report of palladated cationic and anionic heptamethines and are qualitatively reproduced by SAC-CI/HE/cc-pVDZ excited-state calculations (see below and ESI†).²⁹

The S₀ → S₁ transitions of cyanine-like polymethines, including, according to the calculations, the present metallated examples, are generally well-approximated as HOMO-to-LUMO excitations; accordingly, the effect of polymethine chain substituents on the energy of the strong S₀ → S₁ absorption can be rationalised by considering the inductive and resonance effects of the substituents on the HOMO and LUMOs.^{37,38} Depending on the choice of the charge-stabilising end group and the number of methine units, the *meso* methine unit sits on a nodal plane perpendicular to the molecular plane for either the HOMO or the LUMO. For both the present chalcogenopyrylium species and the classes of heptamethines used in our previous report on Pd(PPh₃)₂Cl-substituted dyes,^{23,38-41} the *meso* position lies on a nodal plane in the HOMO (*i.e.*, it is an “unstarred” position in the terminology of the Dewar-Knott rules^{42,43}). Thus, the blue shift suggests that M(PPh₃)₂Cl substituents primarily destabilise the LUMO relative to that of the corresponding Cl compound, due to either stronger π -donor properties and/or weaker σ -acceptor qualities. Electrochemical data (Table 1 and Fig. S8, ESI†) are consistent in that metallation much more significantly affects the reduction potentials than the oxidation potentials. It is worth also noting that the oxidations of **1Pd** and **1Ni** are electrochemically reversible, in contrast to that of **1Cl**; this may be a steric effect, as in previous work on the stability of

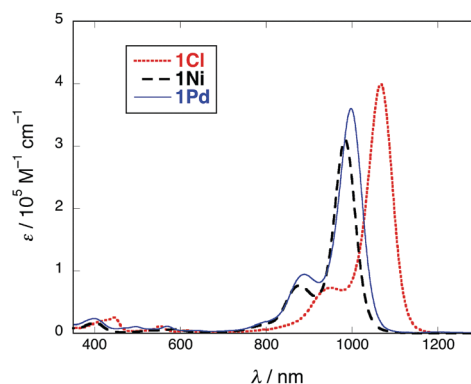
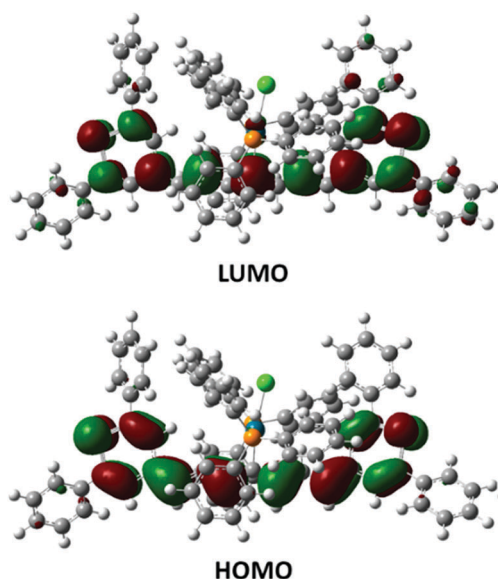


Fig. 1 UV-vis-NIR absorption spectra of Cl- and M(PPh₃)₂Cl-substituted thiopyrylium-terminated heptamethines in chloroform solution.

Table 1 Solution linear and nonlinear optical data (CHCl₃) and electrochemical data (CH₂Cl₂/0.1 M Bu₄NPF₆) for a series of thiopyrylium heptamethines with Cl, Ni(PPh₃)₂Cl, and Pd(PPh₃)₂Cl *meso*-substituents

Dye	λ_{\max}/nm	$\epsilon_{\max}/10^5 \text{ M}^{-1} \text{ cm}^{-1}$	$\mu_{\text{ge}}^a/\text{D}$	$\text{Re}(\gamma)^b/10^{-32} \text{ esu}$	$ \text{Re}(\gamma)/\text{Im}(\gamma) ^b$	$E_{1/2}^{\text{ox}}/V$	$E_{1/2}^{\text{red}}/V$	$\Delta E_{1/2}^d/V$
1Cl	1067	4.0	19.3	-3.2	35	+0.17 ^e	-0.63	0.80
1Ni	984	3.1	16.3	-0.4	6.2	+0.20	-0.87	1.07
1Pd	999	3.6	17.2	-2.4	11.8	+0.20	-0.83	1.03

^a Obtained as $0.0958 \int (\epsilon/\nu) d\nu$ where ϵ and ν are in $\text{M}^{-1} \text{ cm}^{-1}$ and cm^{-1} , respectively, integrating over the $S_0 \rightarrow S_1$ absorption. ^b Z-scan measurements at 1.55 μm (see ESI).^{45,46} The corresponding values of the nonlinear refraction cross-section and 2PA cross-section are -134 and +46 GM, respectively, for **1Ni** and -786 and +140 GM, respectively, for **1Pd**.¹¹ ^c Half-wave potentials vs. FeCp₂⁺⁰ corresponding to oxidation of the cationic dye to a radical dication, or reduction to a neutral radical. ^d Electrochemical gap, $\Delta E_{1/2} = E_{1/2}^{\text{ox}} - E_{1/2}^{\text{red}}$. ^e Irreversible.

**Fig. 2** DFT (ω B97X-D/cc-pVDZ) HOMO and LUMO for **M1Pd**.

the radical dications formed by oxidation of cationic cyanines, where even replacing Me by Et groups can have dramatic effects.⁴⁴

DFT (ω B97X-D/cc-pVDZ) calculations for model compounds (Scheme 2 and Fig. 2; Fig. S3 and S4 in the ESI[†]) confirm the expected nodal properties of the frontier orbitals and indicate, consistent with electrochemistry, that it is indeed the LUMO energy that is more significantly affected by metallation, and that Ni(PPh₃)₂Cl has a slightly more destabilising effect than

Pd(PPh₃)₂Cl (or Pt(PPh₃)₂Cl). Moreover, metal d-orbital contributions to the LUMO (and the HOMO-1) are also evident for the metallated species. They also indicate that the HOMO-LUMO gap for the chloro species is lower than that of the analogous species in which the Cl is replaced by H, consistent with what is seen for indole-terminated heptamethines.³⁸ The DFT polymethine C-C bond lengths also change subtly from Cl to M(PPh₃)₂Cl derivatives, consistent with the M(PPh₃)₂Cl substituents acting as stronger π -donors than the Cl atom (the thiopyrylium-C _{α} and C _{β} -C _{γ} bonds slightly shorten and the C _{α} -C _{β} and C _{γ} -C _{δ} bonds lengthen; see Table S2 in the ESI[†]).

In addition to the *meso*-substituent, the “end” (R) substituent and the choice of chalcogen are also known to affect the spectra of dyes of this type, whereas the “back” (R') group has little effect (as seen here comparing **2Cl** to **1Cl**, or **2Pd** to **1Pd**); within the series **1Cl-5Cl** and **1Pd-5Pd** (see Table 2 and Table S1, ESI[†]) these effects are consistent with previous literature work. Replacement of “end” (R) phenyl groups with alkyl or out-of-plane aryl groups is known to result in a significant blue shift,^{21,26} whereas increasingly heavy chalcogens result in successive red shifts.^{18,19,23,26} These two effects more-or-less cancel when comparing **1Cl/2Cl** to **4Cl** or **1Pd/2Pd** to **4Pd**, as previously seen in the comparison of **1Cbz** to **4Cbz**.²⁶ The additional red shift seen on replacing Se with Te, largely offsets the blue shift engendered by the Pd(PPh₃)₂Cl *meso*-substituent (relative to Cl or 3,6-di-*tert*-butylcarbazol-9-yl groups, the latter exhibiting slightly red-shifted spectra vs. chloro, presumably as a result of limited π -donation from the out-of-plane group and/or weaker inductive electron-withdrawal abilities²⁶), results in **5Pd** exhibiting an absorption maximum (1069 nm) close to that

Table 2 Properties for M(PPh₃)₂Cl-substituted chalcogenopyrylium-terminated heptamethines in high-chromophore-density films compared to those in solution

Dye	CHCl ₃		Neat film		50 wt% with APC		
	λ_{\max}/nm	$\text{FWHM}^a/10^3 \text{ cm}^{-1}$	λ_{\max}/nm	$\text{FWHM}^a/10^3 \text{ cm}^{-1}$	λ_{\max}/nm	$\text{FWHM}^a/10^3 \text{ cm}^{-1}$	$\alpha^b/\text{dB cm}^{-1}$
1Ni	984	0.61	1012	2.64	1005	2.14	^c
1Pd	999	0.66	1024	2.76 ^d	1012	1.06 ^d	6.1
1'Pd	999	0.65	1072	3.29	1048	2.46	10.2
2Pd	999	0.64	1025	2.87	1016	2.17	4.0
3Pd	995	0.61	1015	2.32	1003	2.18	6.5
4Pd	994	0.49	1010	2.27	999	2.10	4.0
5Pd	1069	0.53	1094	2.19	1076	2.14	6.3

^a Full width at half maximum. ^b Linear loss at 1.55 μm obtained using a prism coupler. ^c Not measured. ^d The large difference between the FWHM between the neat film and the blend can be partly attributed to the change in the absorbance of the vibronic sub-band relative to that of the maximum (see Fig. 5).

previously reported for **4Cbz** (1055 nm).²⁶ The similarity of absorption maxima for **3Cl** (1054 nm) and **3Pd** (995 nm) to those of **1Cl/2Cl** (1063 nm) and **1Pd/2Pd** (999 nm), respectively, suggests that the *ortho*-alkynyl substituent of the “end” aryl groups does not result in as effective an out-of-plane twist as the use of 2,6-Me₂C₆H₃ “end” groups.²¹

Solution nonlinear optical properties

The real and imaginary parts of the molecular-level third-order polarisabilities, $\text{Re}(\gamma)$ and $\text{Im}(\gamma)$, were measured at a wavelength of 1.55 μm using the Z-scan technique^{45,46} for **1Pd** and **1Ni** and compared to previously reported data for **1Cl**.²⁶ Trends in the $\text{Re}(\gamma)$ for polymethines can often be rationalised using only the N-term of eqn (1). Indeed, the differences in $\text{Re}(\gamma)$ between **1Cl** and **1Pd** can largely be accounted for by the higher energy, but slightly weaker, $S_0 \rightarrow S_1$ absorption of the latter, along with reduced near-resonance enhancement in the latter case. The reduced value of $|\text{Re}(\gamma)/\text{Im}(\gamma)|$ seen for the **1Pd** species is due to both the reduced magnitude of $\text{Re}(\gamma)$ and to a larger value of $\text{Im}(\gamma)$, arising from a larger 2PA cross-section. The latter effect can also be attributed to the blue shift of the absorption maximum; cyanine-like dyes typically exhibit vibronically assisted $S_0 \rightarrow S_1$ 2PA with peak transition energies *ca.* 0.2 eV greater than the $S_0 \rightarrow S_1$ 1PA peak transition energy and so will more closely approach resonance with 1.55 μm photons as the 1PA is blue-shifted. Indeed, the differences in molecular NLO properties between **1Cl** and **1Pd** are similar to those between **1Cl** and an analogue in which replacement of the phenyl substituents on the thiopyrylium moieties with *tert*-butyl groups is responsible for a blue shift.²⁶

The magnitude of $\text{Re}(\gamma)$ for **1Ni**, on the other hand, is much smaller than that for either **1Cl** or **1Pd** and cannot be rationalised solely by consideration of the $S_0 \rightarrow S_1$ excitation. To investigate the origin of this effect in more detail we turned to SAC-CI/HF/cc-pVDZ excited-state calculations, from the results of which we evaluated $\text{Re}(\gamma_0)$ using the sum-over-states procedure. The excited-state calculations overestimate the difference in $S_0 \rightarrow S_1$ energies between Cl- and Pd(PPh₃)₂Cl-substituted

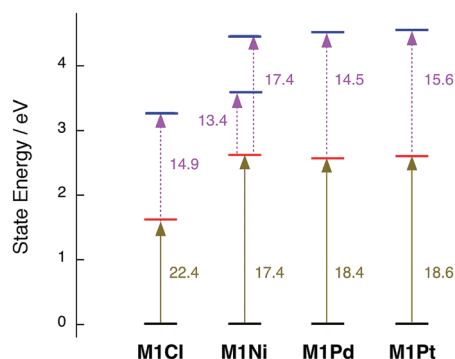


Fig. 3 Partial state-energy diagram for Cl- and M(PPh₃)₂Cl-substituted thiopyrylium-terminated heptamethines from SAC-CI/HF/cc-pVDZ calculations. Transition moments are shown (in Debye) for the $g \rightarrow e$ ($S_0 \rightarrow S_1$) 1PA transitions (solid arrows) and $e \rightarrow e'$ transitions (where $g \rightarrow e'$ are 2PA-allowed transitions).

examples and, therefore, overestimate the difference in $\text{Re}(\gamma)$ (Fig. 3; Tables S3 and S4, ESI[†]). Nevertheless, for **M1Cl** and **M1Pd** (and **M1Pt**), the N-term associated with $S_0 \rightarrow S_1$ dominates the sum-over-states value of $\text{Re}(\gamma_0)$ (Table S4, ESI[†]). The T-terms are comparatively small since the lowest energy e' states are 1.7–2.0 times higher in energy than S_1 . On the other hand, calculations for **M1Ni** reveal not only a significant T-term contribution from S_3 at an energy 1.7 times that of S_1 , but also from S_2 at only 1.4 times the energy of S_1 ; together these outweigh the N-term to afford a small positive value of $\text{Re}(\gamma_0)$ (experiment affords a small negative value of $\text{Re}(\gamma)$ at 1.55 μm ; this discrepancy can easily arise if the calculations do not afford precisely correct relative state energies or transition dipoles). The origin of this effect is not particularly straightforward: both S_2 and S_3 of **M1Ni** arise primarily from linear combinations of (HOMO) \rightarrow (LUMO+1), (HOMO–1) \rightarrow (LUMO), and double (HOMO \rightarrow LUMO) electronic excitations, as do the S_2 states of **M1Cl**, **M1Pd**, and **M1Pt**, and these orbitals are all typical polymethine π -orbitals to which the *meso* substituents make only relatively minor contributions (as shown in Fig. S3, ESI[†]; it is the HOMO–2 and LUMO+2 in which large differences in the orbital distributions become evident between the different substituents). However, regardless of the detailed reasons for the differences between Ni(PPh₃)₂Cl- and Pd(PPh₃)₂Cl-species, the small magnitudes of $\text{Re}(\gamma)$ found and calculated for the former emphasise the importance of taking into account the properties of higher lying excited states besides S_1 when identifying cyanine-like dyes for third-order NLO applications. In particular, it is important to realise that a cyanine-like molecular structure and a cyanine-like absorption spectrum do not necessarily guarantee typical cyanine-like NLO behaviour (*i.e.*, large negative $\text{Re}(\gamma)$ and, therefore, nonlinear refractive index, n_2).

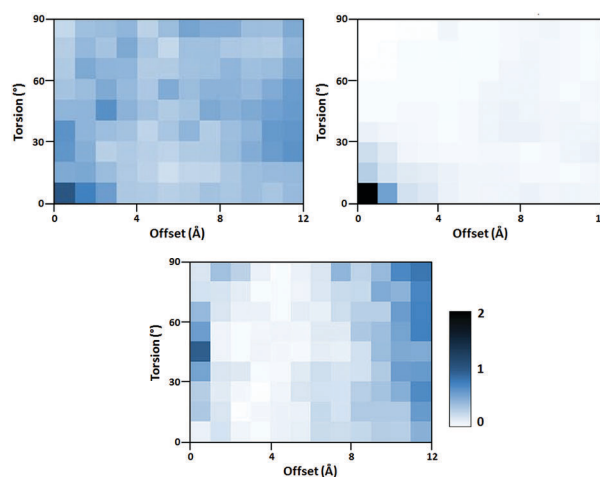


Fig. 4 Aggregate geometries probability distribution for **M1H** with BF₄[−] (top left) and BAR₄' (top right) counterions and for **M1Pd** (Cl counterion, bottom) using the same methods as our previous work.^{26,47,48} The color scale on the lower right corresponds to the probability of finding aggregates, with the probability of 1 corresponding to the average bulk density of thiopyrylium pairs.

Modeling of effects on M(PPh₃)₂Cl groups on aggregation

To gain insight into the possible impact of bulky M(PPh₃)₂Cl groups on aggregation in amorphous neat films of chalcogenopyrylium-terminated dyes, we performed atomistic molecular dynamics simulations as previously described for other polymethine systems.^{26,47,48} Fig. 4 shows the probabilities of obtaining different dye–dye aggregates, defined as pairs of chromophores separated by a radial distance of 6 Å or less, for the **M1H** cation with BF₄⁻ and BAR₄'⁻ anions and for **M1Pd** with Cl⁻ anions. For **M1H**-BAR₄'⁻ the preferred aggregate geometries consist of parallel molecules with little or no lateral offset, thus approaching the ideal “H-aggregate” geometry. On the other hand, **M1H**-BF₄⁻ forms a much wider range of aggregate geometries. These findings are broadly consistent with absorption spectra for **1Cl** and **1Cl'**, which are respectively blue-shifted (H-aggregate-like) and red-shifted (yet much broader than expected for simple J-type aggregation).⁶ Even with the small chloride counterion, the bulky *meso*-substituent of **M1Pd** is predicted to preclude many of the aggregate geometries adopted by **M1H**-BF₄⁻, including both H-aggregates and, to a large extent, J-aggregates, although the plot shows a significant probability of zero-offset aggregates clustered around a twist angle of *ca.* 45°, as well as the possibility of aggregates with large offsets and a variety of torsion angles.

Solid-state optical properties

Solid-state UV-vis-NIR absorption spectra were acquired for the M(PPh₃)₂Cl-functionalised dyes as both neat films and as 50 wt% blends with amorphous polycarbonate (APC). In all cases, the maxima are bathochromically shifted relative to those seen in solution, the absorption feature is considerably broader, and the vibronic shoulder is increased in relative absorbance. Nonetheless, to a first approximation, the spectra of all the M(PPh₃)₂Cl-functionalised dyes are reasonably solution-like and do not show marked H- or J-aggregate-like features. In contrast, as noted above, **1Cl** (Fig. 5) and **1Cl'** exhibit spectra that strongly deviate from those found in solution.^{6,25} The Pd(PPh₃)₂Cl group in **1Pd** is also more effective in narrowing the absorption band in the solid than the bulky and rigidly out-of-plane 3,6-di-*tert*-butylcarbazol-9-yl *meso*-substituent in the previously reported **1Cbz**, which exhibits a significant J-aggregate-like low-energy shoulder in solid films (Fig. 5).²⁶ In our previous work, the 3,6-di-*tert*-butylcarbazol-9-yl group was more efficient at affording solution-like spectra in films when combined with a bulky “back” (R' in Scheme 1) substituent, such as the ^tBu group used in **4Cbz** and, more importantly, in combination with out of plane tertiary alkyl “end”-substituents (R in Scheme 1).²⁶ Moreover, in contrast to **4Cbz** and related compounds, **1Pd** is accessible through two simple steps (counterion metathesis and reaction with Pd(PPh₃)₄) from a commercially available material (**1Cl**, IR1061). Even **1Pd** (only a single step from **1Cl**) exhibits a solution-like spectrum, although the use of the smaller BF₄⁻ counterion results in a broader overall absorption than that of **1Pd** (Table 2). The ^tBu substituent of **2Pd** has little impact on the solid-state spectra. The out-of-plane “end” groups of **3Pd**-**5Pd** result in absorption bands in neat films (Table 2) that are slightly narrower than those of the

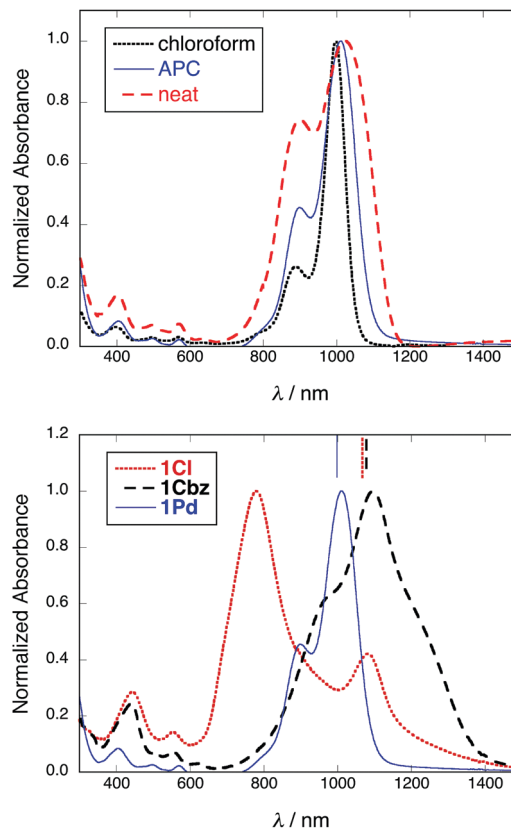


Fig. 5 Top: UV-vis-NIR absorption spectra for **1Pd** in dilute chloroform solution and in 50 wt% and 100 wt% films. Bottom: UV-vis-NIR absorption spectra of Cl⁻, 3,6-di-*tert*-butylcarbazol-9-yl-, and Pd(PPh₃)₂Cl-substituted thiopyrylium-terminated heptamethines as 50 wt% blends with APC. The vertical marks on the upper X-axis of this plot indicate the positions of the corresponding absorption maxima in CHCl₃.

compounds with Ph “end” groups (R) or than that of **4Cbz** (for which FWHM = 2880 cm⁻¹).

Linear optical losses were also measured for selected films of 1:1 blends with APC at 1550 nm using a prism coupler (Table 2). Of the blends examined, the loss for **1Pd** (which also exhibits the broadest absorption band) is the highest. The values for the other blends fall in a similar range to those for some previous examples of chalcogenopyrylium-terminated polymethines with bulky *meso*-substituents (*e.g.*, 8.5 and 4.4 dB cm⁻¹ for **1Cbz** and **4Cbz**, respectively, as 1:1 blends with APC), although they are all somewhat higher than the best previously reported values (3.3–3.5 dB cm⁻¹ for thiopyrylium examples with tertiary alkyl “end” groups, a ^tBu “back” group, and a 3,6-di-*tert*-butylcarbazol-9-yl *meso*-substituent).^{26,27}

Finally, the real part of the third-order susceptibility, Re(χ⁽³⁾), for a 1:1 **5Pd**:APC blend was measured using the Z-scan method to be -3×10^{-11} esu, a value which is close to that of -3.3×10^{-11} esu previously found for a 1:1 blend of **4Cbz** (which, as noted above, exhibits similar linear spectra to **5Pd**) and APC. The 2PA figure-of-merit, $|\text{Re}(\chi^{(3)})/\text{Im}(\chi^{(3)})|$, was estimated to be greater than 10 (*cf.* a value of 12 for **4Cbz**). These values, combined with the optical loss value of 6.3 dB cm⁻¹, suggest that, with further optimisation of processing and film

blending, **5Pd**, and perhaps other Pd(PPh₃)₂Cl-substituted chalcogenopyrylium-terminated heptamethines, may be viable candidates for all-optical signal-processing applications in high-chromophore-density films.

Conclusions

M(PPh₃)₂Cl-functionalisation of chalcogenopyrylium-terminated polymethines is an effective means of reducing dye-dye interactions in the solid state, as previously demonstrated for other classes of dyes. Metal substitution does not affect the cyanine-like character of the absorption spectra. For a Pd example, the third-order NLO properties are typically cyanine-like, but for a Ni example, the magnitude of the nonlinearity is considerably reduced owing to the contributions of a low-lying 2PA state, illustrating that chromophores with cyanine-like absorption spectra do not necessarily also exhibit cyanine-like NLO properties. A Pd example with telluropyrylium termini exhibits solid-state NLO properties and linear loss values that are promising for use in near-IR all-optical switching applications.

Conflicts of interest

There are no conflicts of interest to declare.

Acknowledgements

This work was supported by the Air Force Office of Scientific Research through the COMAS MURI program (Agreement no. FA9550-10-1-0558). We thank Hyeongeun Kim for help with preliminary spectroscopic measurements on films.

References

- 1 A. Mishra, R. K. Behera, P. K. Behera, B. K. Mishra and G. B. Behera, *Chem. Rev.*, 2000, **100**, 1973.
- 2 T. Tani, in *J-Aggregates*, ed. T. Kobayashi, World Scientific, Singapore, 1996.
- 3 B. A. Armitage, *Top. Curr. Chem.*, 2005, **253**, 55.
- 4 I.-I. S. Lim, F. Goroleski, D. Mott, N. Kariuki, W. Ip, J. Luo and C. J. Zhong, *J. Phys. Chem. B*, 2006, **110**, 6673–6682.
- 5 L. A. King and B. A. Parkinson, *Langmuir*, 2017, **33**, 468.
- 6 J. M. Hales, S. Barlow, H. Kim, S. Mukhopadhyay, J.-L. Brédas, J. W. Perry and S. R. Marder, *Chem. Mater.*, 2014, **26**, 549.
- 7 M. Hochberg, T. Baehr-Jones, G. X. Wang, M. Shearn, K. Harvard, J. D. Luo, B. Q. Chen, Z. W. Shi, R. Lawson, P. Sullivan, A. K. Y. Jen, L. Dalton and A. Scherer, *Nat. Mater.*, 2006, **5**, 703.
- 8 C. Koos, P. Vorreau, T. Vallaitis, P. Dumon, W. Bogaerts, R. Baets, B. Esembeson, I. Biaggio, T. Michinobu, F. Diederich, W. Freude and J. Leuthold, *Nat. Photonics*, 2009, **3**, 216.
- 9 V. Mizrahi, K. W. DeLong, G. I. Stegeman, M. A. Saifi and M. J. Andrejco, *Opt. Lett.*, 1989, **14**, 1140.
- 10 B. J. Orr and J. F. Ward, *Mol. Phys.*, 1971, **20**, 513.
- 11 T. R. Ensley, H. Hu, M. Reichert, M. R. Ferdinandus, D. Peceli, J. M. Hales, J. W. Perry, Z. Li, S.-H. Jang, A. K.-Y. Jen, S. R. Marder, D. J. Hagan and E. W. Van Stryland, *J. Opt. Soc. Am. B*, 2016, **33**, 780 (Erratum: *J. Opt. Sci. Am. B*, 2016, **33**, 1007).
- 12 J. L. Bricks, A. D. Kachkovskii, Y. L. Slominskii, A. O. Gerasov and S. V. Popov, *Dyes Pigm.*, 2015, **121**, 238.
- 13 J. S. Craw, J. R. Reimers, G. B. Bacskey, A. T. Wong and N. S. Hush, *Chem. Phys.*, 1992, **167**, 77.
- 14 L. M. Tolbert and X. Zhao, *J. Am. Chem. Soc.*, 1997, **119**, 3253.
- 15 S. L. Lepkowicz, O. V. Przhonska, J. M. Hales, J. Fu, D. J. Hagan, E. W. Van Stryland, M. V. Bondar, Y. L. Slominsky and A. D. Kachkovski, *Chem. Phys.*, 2004, **305**, 259.
- 16 A. D. Kachkovski, M. A. Kudinova, B. I. Shapiro, N. A. Derevjanko, L. G. Kurkina and A. I. Tolmachev, *Dyes Pigm.*, 2005, **64**, 207.
- 17 O. V. Przhonska, H. Hu, S. Webster, J. L. Bricks, A. A. Vinichuk, A. D. Kachkovski and Y. L. Slominsky, *Chem. Phys.*, 2013, **411**, 17.
- 18 A. I. Tolmachev and M. A. Kudinova, *Chem. Heterocycl. Compd.*, 1974, **10**, 41.
- 19 M. R. Detty and B. J. Murray, *J. Org. Chem.*, 1982, **47**, 5235.
- 20 A. D. Kachkovski, M. A. Kudinova, B. I. Shapiro, N. A. Derevjanko, L. G. Kurkina and A. I. Tolmachev, *Dyes Pigm.*, 1984, **5**, 295.
- 21 J. Panda, P. R. Virkler and M. R. Detty, *J. Org. Chem.*, 2003, **68**, 1804.
- 22 M. A. Bedics, H. Kearns, J. M. Cox, S. Mabbott, F. Ali, N. C. Shand, K. Faulds, J. B. Benedict, D. Graham and M. R. Detty, *Chem. Sci.*, 2015, **6**, 2302.
- 23 J. M. Hales, J. Matichak, S. Barlow, S. Ohira, K. Yesudas, J.-L. Brédas, J. W. Perry and S. R. Marder, *Science*, 2010, **327**, 1485.
- 24 S. Mukhopadhyay, C. Risko, S. R. Marder and J. L. Brédas, *Chem. Sci.*, 2012, **3**, 3103.
- 25 A. Scarpaci, A. Nantalaksakul, J. M. Hales, J. D. Matichak, S. Barlow, M. Rumi, J. W. Perry and S. R. Marder, *Chem. Mater.*, 2012, **24**, 1606.
- 26 S. Barlow, J.-L. Brédas, Y. A. Getmanenko, R. L. Gieseck, J. M. Hales, H. Kim, S. R. Marder, J. W. Perry, C. Risko and Y. Zhang, *Mater. Horiz.*, 2014, **1**, 577.
- 27 Y. A. Getmanenko, T. G. Allen, H. Kim, J. M. Hales, B. Sandhu, M. S. Fonari, K. Y. Suponitsky, Y. Zhang, V. N. Khrustalev, J. D. Matichak, T. V. Timofeeva, S. Barlow, S.-H. Chi, J. W. Perry and S. R. Marder, in preparation.
- 28 S. Shahin, K. Kieu, J. M. Hales, H. Kim, Y. A. Getmanenko, Y. Zhang, J. W. Perry, S. R. Marder, R. A. Norwood and N. Peyghambarian, *J. Opt. Soc. Am. B*, 2014, **31**, 2455.
- 29 I. Davydenko, S. Barlow, R. Sharma, S. Benis, J. Simon, T. G. Allen, M. W. Cooper, V. Khrustalev, E. V. Jucov, R. Castañeda, C. Ordonez, Z. Li, S.-H. Chi, S.-H. Jang, T. C. Parker, T. V. Timofeeva, J. W. Perry, A. K.-Y. Jen, D. J. Hagan, E. W. Van Stryland and S. R. Marder, *J. Am. Chem. Soc.*, 2016, **138**, 10112.

- 30 H. Weissman, E. Shirman, T. Ben-Moshe, R. Cohen, G. Leitus, L. J. W. Shimon and B. Rybtchinski, *Inorg. Chem.*, 2007, **46**, 4790.
- 31 Z. Feng, L. Jiao, Y. Feng, C. Yu, N. Chen, Y. Wei, X. Mu and E. Hao, *J. Org. Chem.*, 2016, **81**, 6281.
- 32 We have also found that the same reagent, Pd(PPh₃)₄, can also catalyse the Stille reaction of meso-Cl dyes, including **4Cl**, with 9-(tributylstannyl)anthracene derivative in the presence of CuI at elevated temperatures (ref. 27). Presumably species such as **4Pd** are intermediates in the catalytic cycle.
- 33 Y. Nagao, T. Osawa, K. Kozawa and T. Urano, *Shikizai Kyokaishi*, 2005, **78**, 12.
- 34 R. Wizinger and H. J. Angliker, *Helv. Chim. Acta*, 1966, **49**, 2046.
- 35 The ³¹P spectrum of **5Pd** in CHCl₃ consists of only a singlet, presumably due to a coincidence in the chemical shifts of the two resonances. However, two doublets are seen in other solvents (e.g., in CD₂Cl₂: δ 16.4 (d, J_{PP} = 305 Hz), 15.1 (d, J_{PP} = 304 Hz)).
- 36 R. G. Goodfellow, *Chem. Commun.*, 1968, 114.
- 37 J. Fabian and H. Hartmann, *Light Absorption of Organic Colorants – Theoretical Treatment and Empirical Rules*, Springer-Verlag, Berlin, 1980.
- 38 J. D. Matichak, J. M. Hales, S. Barlow, J. W. Perry and S. R. Marder, *J. Phys. Chem. A*, 2011, **115**, 2160.
- 39 K. Yesudas, *Phys. Chem. Chem. Phys.*, 2013, **15**, 19465.
- 40 Y. L. Slominsky, A. D. Kachkovski, S. V. Popov, L. A. Nechitailo and N. V. Ignatiev, *Dyes Pigm.*, 1991, **15**, 247.
- 41 Ref. 23 and 39 show frontier molecular orbitals for chalcogenopyrylium-terminated heptamethines, which are similar to those obtained here for **M1Cl**, **M1Ni**, **M1Pd**, and **M1Pt**. Ref. 39 and 40 show MOs previously calculated for indoline, benzothiazole, and dicyanomethylene-terminated polymethines, which serve as models for the benzoindoline, naphthothiazole, and “TCF”-terminated species studied in ref. 29, with the understanding that the HOMOs of mono-, penta-, nona-, and tridecamethines will have the same nodal properties as one another and as the LUMOs of tri-, hepta-, and undecamethines, the LUMOs of the former class will resemble the HOMOs of the latter, and that TCF-terminated heptamethines are effectively C(CN)₂-terminated tridecamethines.
- 42 M. J. S. Dewar, *J. Chem. Soc.*, 1950, 2329.
- 43 E. B. Knott, *J. Chem. Soc.*, 1951, 1024.
- 44 J. R. Lenhard and A. D. Cameron, *J. Phys. Chem.*, 1993, **97**, 4916.
- 45 M. R. Ferdinandus, M. Reichert, T. R. Ensley, H. Hu, D. A. Fishman, S. Webster, D. J. Hagan and E. W. Van Stryland, *Opt. Mater. Express*, 2012, **2**, 1776.
- 46 M. Sheik-Bahae, A. A. Said, T.-H. Wei, D. J. Hagan and E. W. Van Stryland, *IEEE J. Quantum Electron.*, 1990, **26**, 760.
- 47 R. L. Gieseking, S. Mukhopadhyay, C. Risko, S. R. Marder and J.-L. Brédas, *Chem. Mater.*, 2014, **26**, 6439.
- 48 R. L. Gieseking, S. Mukhopadhyay, S. B. Shiring, C. Risko and J.-L. Brédas, *J. Phys. Chem. C*, 2014, **118**, 23575.